eLIFE elifesciences.org

RESEARCH ARTICLE

Figures and figure supplements

LEAFY maintains apical stem cell activity during shoot development in the fern *Ceratopteris richardii*

Andrew RG Plackett *et al*

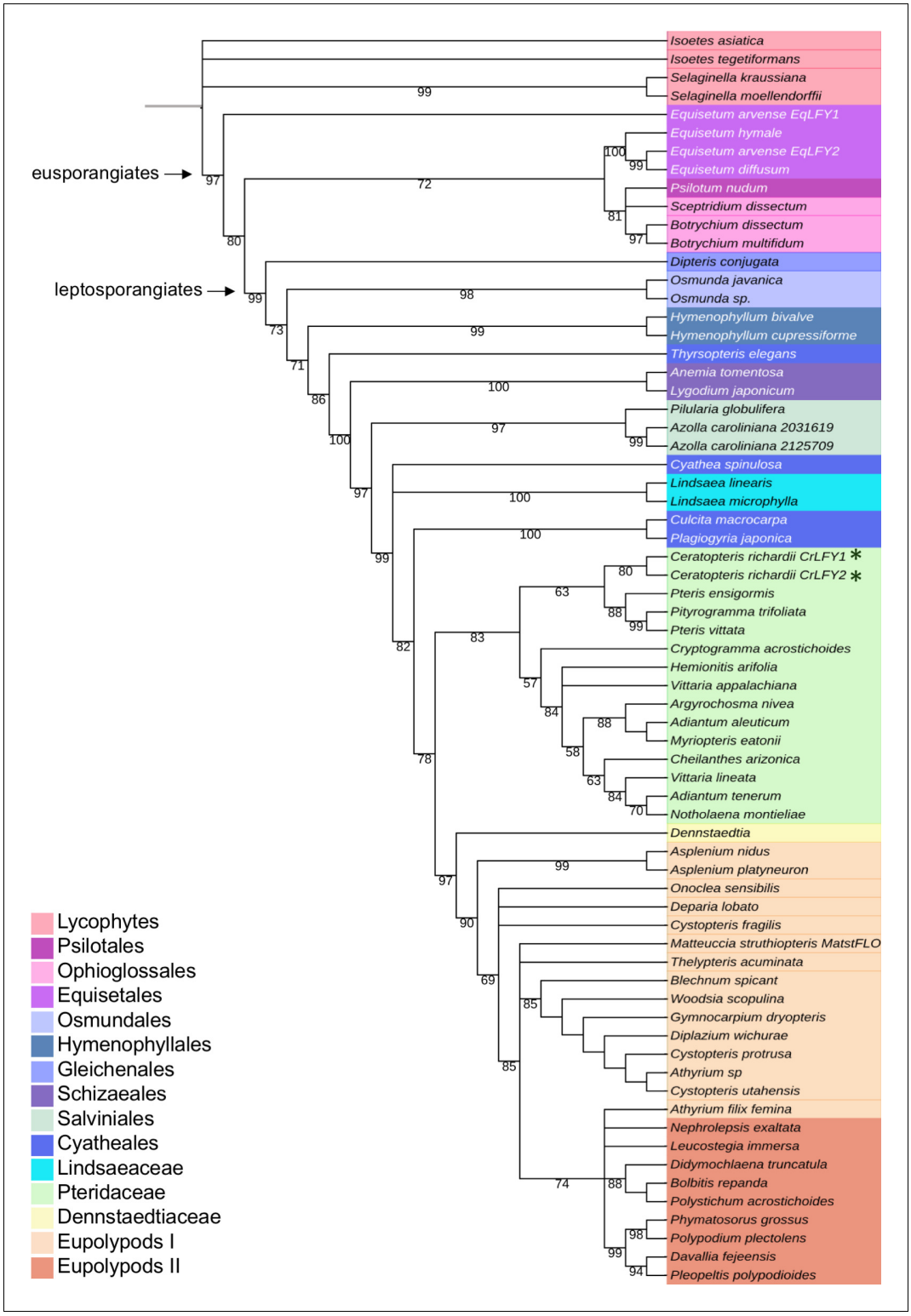

Figure 1. *CrLFY1* and *CrLFY2* arose from a recent gene duplication event. Inferred phylogenetic tree from maximum likelihood analysis of 64 LFY amino acid sequences (see ***Supplementary file 1*** for accession numbers) sampled from within the fern lineage plus lycophyte sequences as an outgroup. Bootstrap values are given for each node. The tree shown is extracted from a phylogeny with representative sequences from all land plant lineages (***Figure 1—figure supplement 1***). The *Ceratopteris richardii* genome contains no more than two copies of LFY (***Figure 1—figure supplement 2***; indicated by *). Different taxonomic clades within the fern lineage are

Figure 1 continued on next page

Figure 1 continued

denoted by different colours, as shown. The divergence between eusporangiate and leptosporangiate ferns is indicated by arrows.

DOI: https://doi.org/10.7554/eLife.39625.003

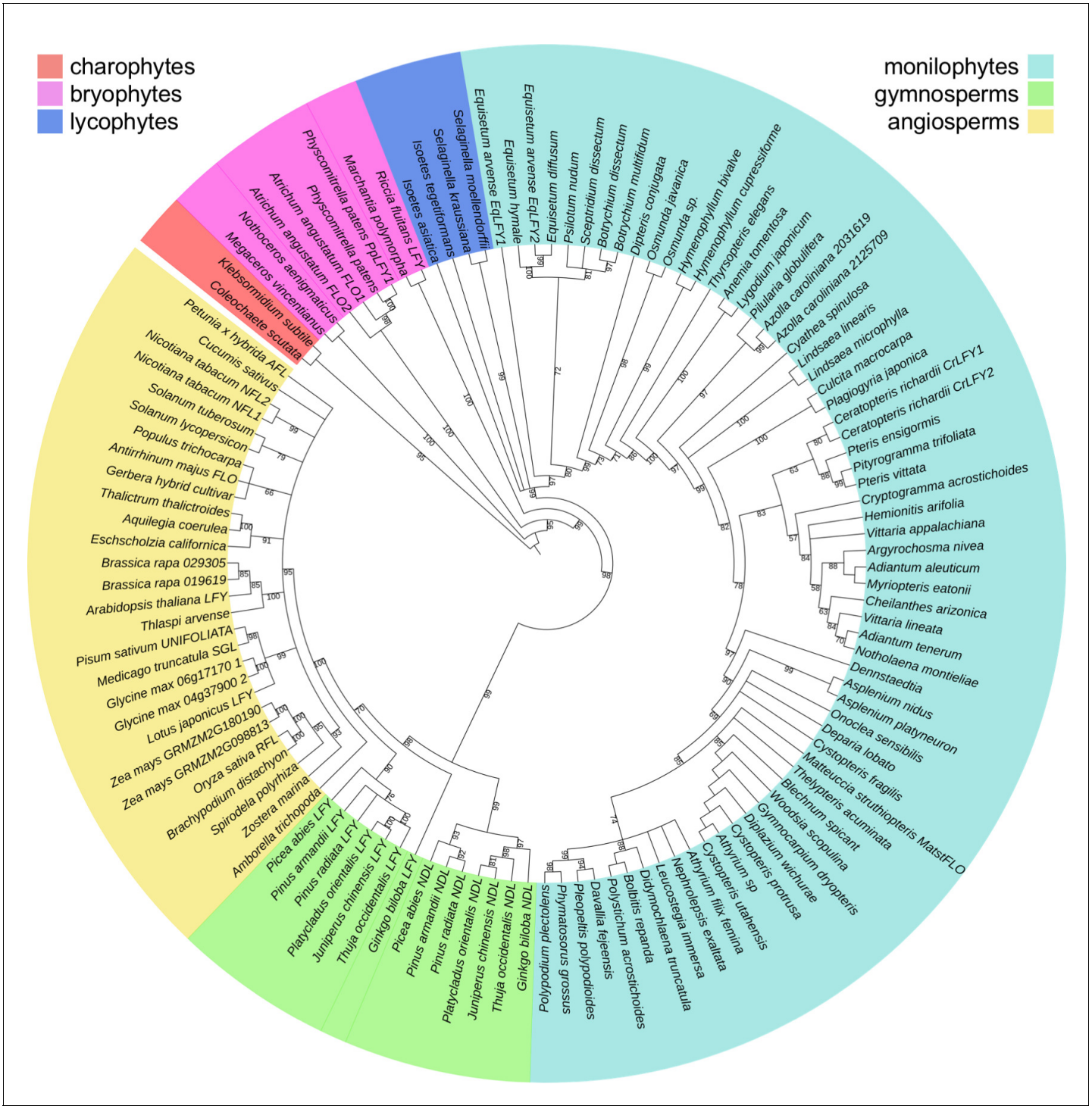

Figure 1—figure supplement 1. Phylogenetic relationships between *LEAFY* sequences reflect established relationships within vascular plant lineages. Inferred phylogenetic tree from maximum likelihood analysis of 120 LFY sequences sampled from across extant land plant lineages (liverworts, mosses, hornworts, lycophytes, monilophytes i.e. ferns and allies, gymnosperms, angiosperms) including algal (charophyte) sequences as an outgroup. Bootstrap values are given for each node. Sequences belonging to each lineage are denoted by different colours, as shown. The higher-order topology between vascular plant lineages (lycophytes, monilophytes, gymnosperms and angiosperms) is consistent with expected relationships; a gene duplication event resulting in *LFY* and *NEEDLY* clades in gymnosperms has been identified previously (***Sayou et al., 2014***); and relationships between bryophyte lineages are consistent with differences in the LFY DNA binding site preference, where hornworts and mosses each differ from the preferred site shared by liverworts and vascular plants (***Sayou et al., 2014***).

DOI: https://doi.org/10.7554/eLife.39625.004

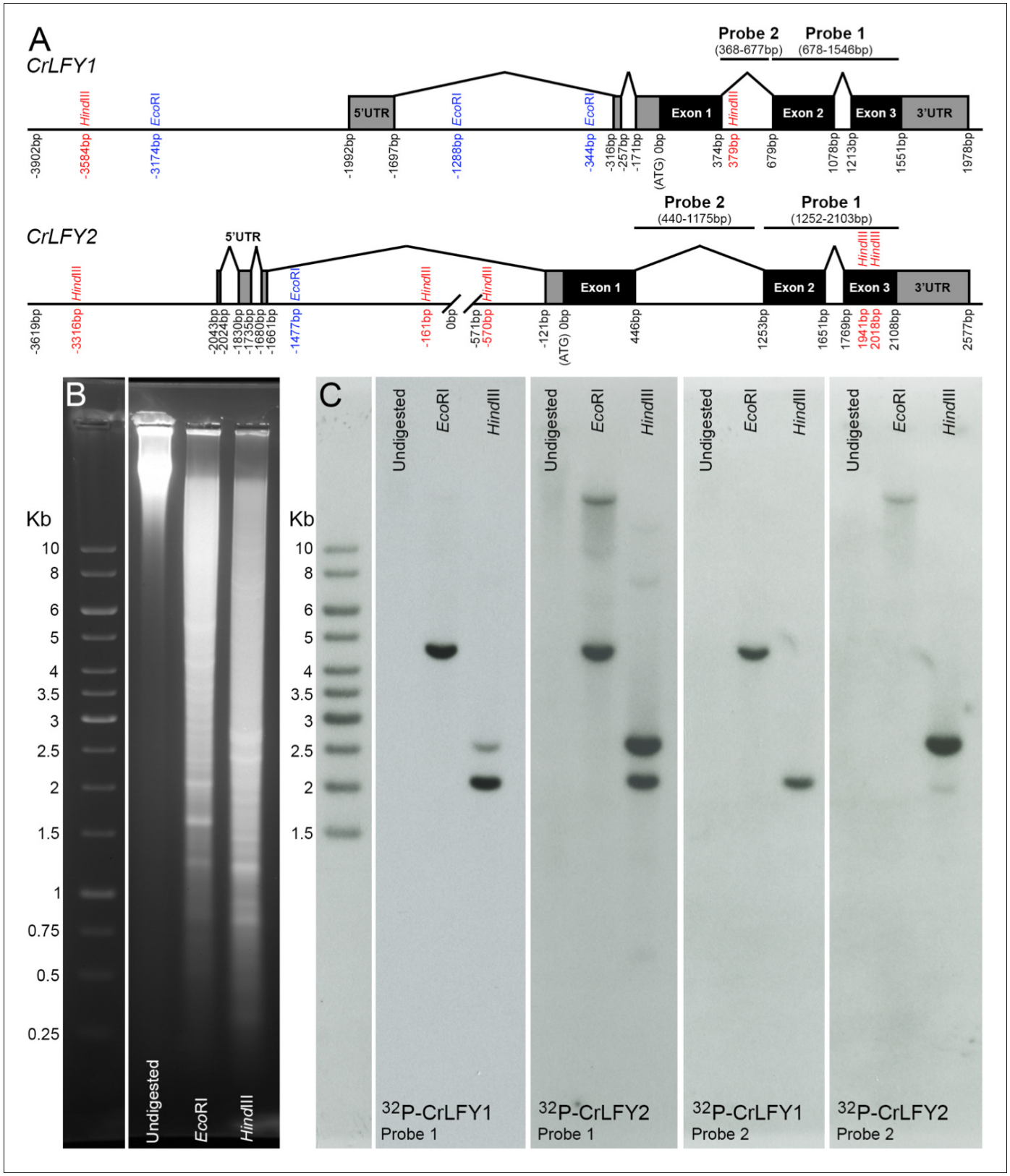

Figure 1—figure supplement 2. The *Ceratopteris* genome contains only two copies of *LFY*. (**A**) Deduced gene structure of *CrLFY1* and *CrLFY2* loci. All positions marked are given relative to the ATG start codon. Hybridization probes used in DNA gel blot analysis and relevant restriction sites (*Eco*RI, *Hind*III) are marked. *CrLFY1* probe 1 (868bp) and *CrLFY2* probe 1 (851bp) share 79% sequence similarity and hybridize to exons 2 + 3 of each gene

Figure 1—figure supplement 2 continued on next page

Figure 1—figure supplement 2 continued

(comprising the conserved LFY DNA binding domain). As such, both probes should hybridize to all members of the *LFY* gene family. *CrLFY1* probe 2 (309bp) and *CrLFY2* probe 2 (735bp) hybridize to intron 1 of each gene copy and share no significant sequence similarity. As such, each probe is expected to hybridize to the specific gene copy. (**B, C**) Gel blot analysis of wild-type genomic DNA, digested with *Eco*RI or *Hind*III, electrophoresed on an ethidium bromide stained gel (**B**), blotted to nylon membrane and hybridized against different probes (**C**) as described in (**A**). *Eco*RI digestion was predicted to generate single hybridizing fragments for both *CrLFY1* and *CrLFY2*, each spanning both probes with minimum expected fragment sizes of ~2.0 kb and ~3.1 kb, respectively. *Hind*III digestion was predicted to generate a single *CrLFY1* hybridizing fragment recognized by both probes with a minimum size of ~1.6 kb. *Hind*III digestion was predicted to generate a *CrLFY2* fragment of ~2.5 kb hybridizing to probes 1 and 2, a separate fragment with a minimum size of 559 bp overlapped by 85 bp of probe 1 (and so potentially undetectable) plus an undetectable fragment of 11 bp. The hybridization patterns observed (**C**) are consistent with these predictions, with the exon probes cross-hybridizing to predicted fragments of both gene copies (but not to any additional gene fragments) and the intron probes primarily hybridizing to the respective specific gene copy.

DOI: https://doi.org/10.7554/eLife.39625.005

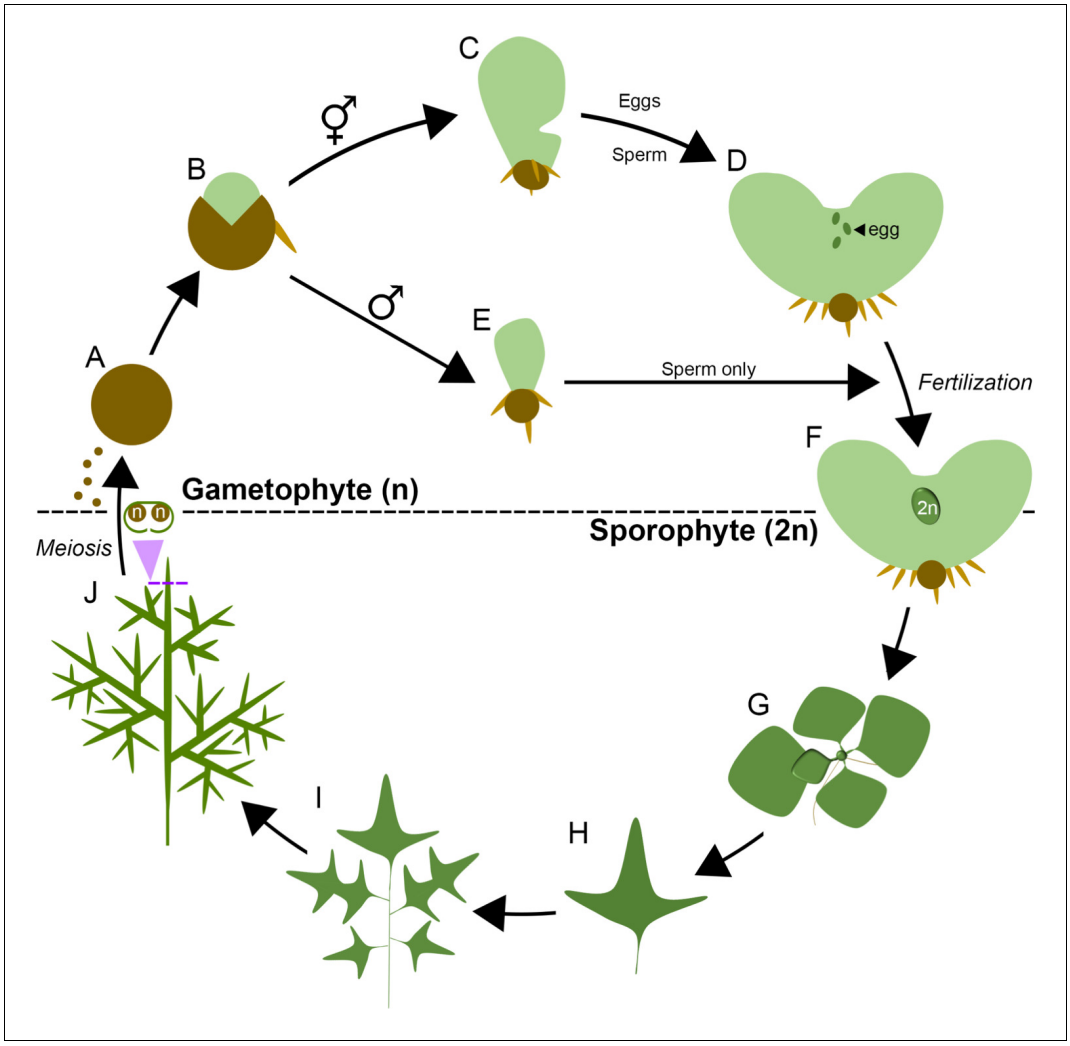

Figure 2. The lifecycle of *Ceratopteris richardii*. Ceratopteris propagates in the haploid gametophyte phase of its lifecycle (**n**) through single-celled spores (**A**) On spore germination (**B**) a two-dimensional photosynthetic thallus develops into one of two sexes, a default hermaphrodite (**C**) which produces eggs and sperm (**D**) or a hormone-induced male that produces sperm only (**E**). Eggs are retained on the hermaphrodite thallus, and fertilization results in the development of a diploid (2n) embryo on the gametophyte (**F**), initiating the sporophyte phase of the lifecycle. The sporophyte establishes a vegetative shoot that initiates leaflike lateral organs (fronds) and roots from its apex (**G**). The first fronds produced are simple but later fronds become increasingly lobed and dissected (**H, I**). The sporophyte undergoes a reproductive phase-change and subsequent fronds generate haploid spores by meiosis on their undersides (**J**), enclosed in a morphologically-distinct curled lamina. Mature spores are dispersed to restart the lifecycle.

DOI: https://doi.org/10.7554/eLife.39625.006

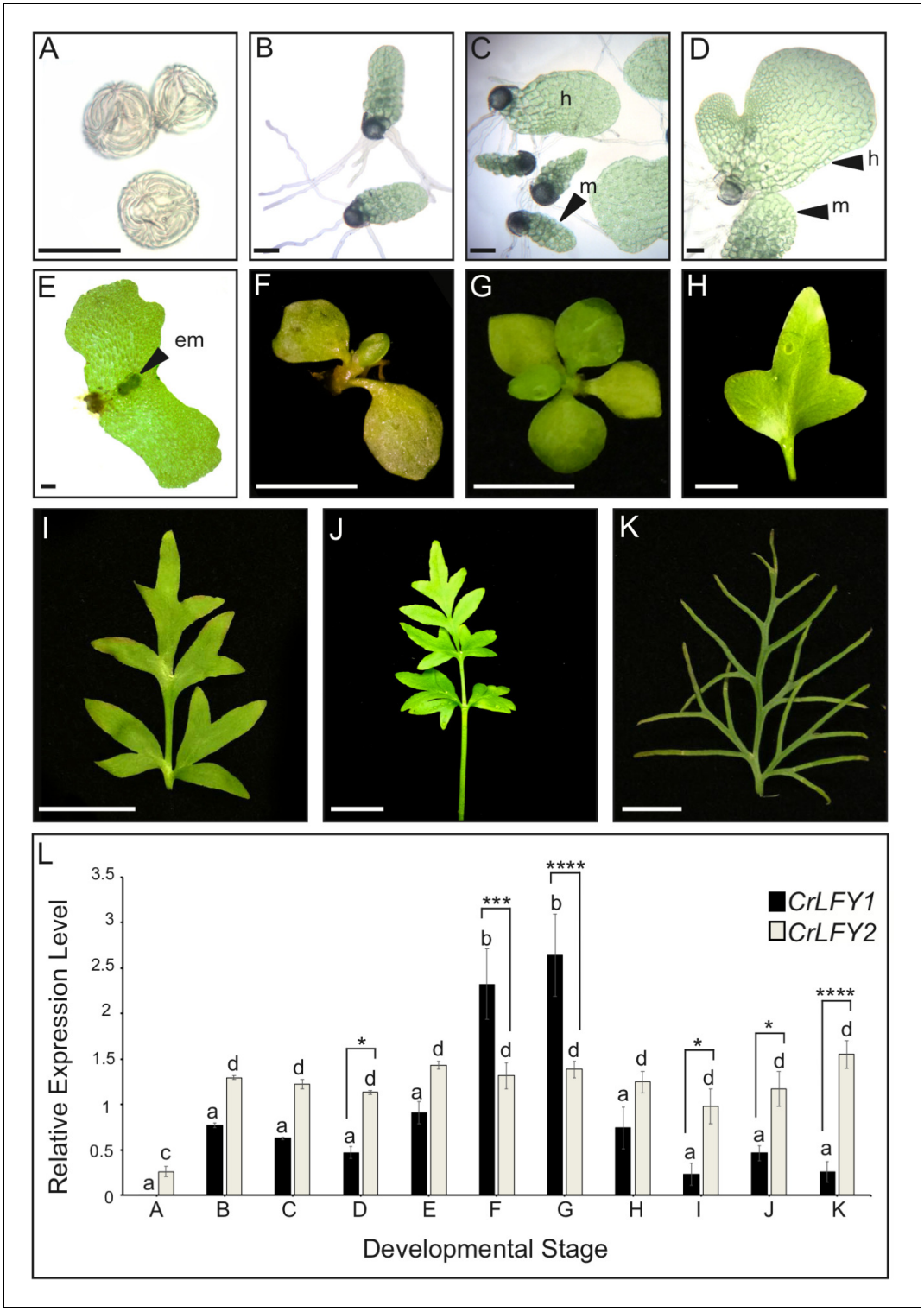

Figure 3. *CrLFY1* and *CrLFY2* are differentially expressed during the Ceratopteris lifecycle. (**A-K**) Representative images of the developmental stages sampled for expression analysis in (**L**). Imbibed spores (**A**); populations of developing gametophytes harvested at 5 (**B, C**) and 8 (**D**) days after spore-sowing (DPS), comprising only males (**B**) or a mixture of hermaphrodites (**h**) and males (**m**) (**C, D**); fertilized gametophyte subtending a developing sporophyte embryo (em) (**E**); whole sporophyte shoots comprising the shoot apex with 3 (**F**) or five expanded entire fronds attached (**G**); individual vegetative fronds demonstrating a heteroblastic progression in which frond complexity increases through successive iterations of lateral outgrowths (pinnae) (**H–J**); complex fertile frond with

Figure 3 continued on next page

Figure 3 continued

sporangia on the underside of individual pinnae (**K**). Scale bars = 100 um (**A–E**), 5 mm (**F–H**), 20 mm (**I–K**). (**L**) Relative expression levels of *CrLFY1* and *CrLFY2* (normalized against the housekeeping genes *CrACTIN1* and *CrTBP*) at different stages of development. *n* = 3; Error bars = standard error of the mean (SEM). Pairwise statistical comparisons (ANOVA followed by Tukey's multiple comparisons test– ***Supplementary file 4***) found no significant difference in *CrLFY2* transcript levels between any gametophyte or sporophyte tissues sampled after spore germination ($p>0.05$) and no significant difference between *CrLFY1* and *CrLFY2* transcript levels during early gametophyte development ($p>0.05$) (**B, C**). Differences between *CrLFY1* and *CrLFY2* transcript levels were significant in gametophytes at 8 DPS ($p<0.05$) (**D**). *CrLFY1* transcript levels were significantly higher in whole young sporophytes (**F**) and vegetative shoots (**G**) compared to isolated fronds (**H–K**) ($p<0.05$). *CrLFY1* transcript levels in whole sporophytes and shoots were greater than *CrLFY2*, whereas in isolated fronds *CrLFY1* transcript levels were consistently lower than *CrLFY2* ($p<0.05$). Asterisks denote significant difference (*, $p<0.05$; **, $p<0.01$, ***, $p<0.001$; ****, $p<0.0001$) between *CrLFY1* and *CrLFY2* transcript levels (Sidak's multiple comparisons test) within a developmental stage. Letters denote significant difference ($p<0.05$) between developmental stages for *CrLFY1* or *CrLFY2* (Tukey's test). Groups marked with the same letter are not significantly different from each other ($p>0.05$). Statistical comparisons between developmental stages were considered separately for *CrLFY1* and *CrLFY2*. The use of different letters between *CrLFY1* and *CrLFY2* does not indicate a significant difference.

DOI: https://doi.org/10.7554/eLife.39625.007

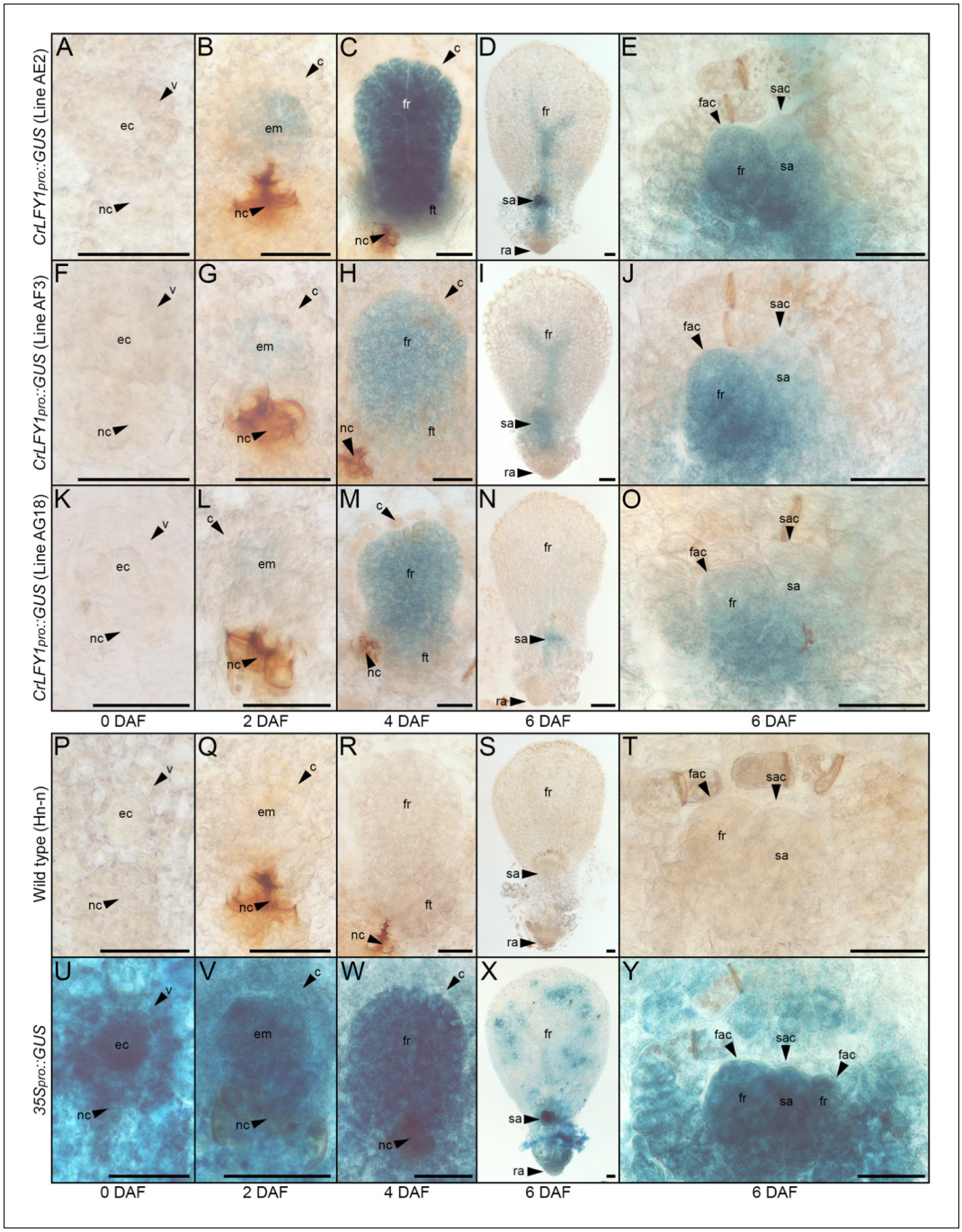

Figure 4. The *CrLFY1* promoter drives reporter gene expression in proliferating tissues of the developing Ceratopteris embryo. (**A–Y**) GUS activity detected as blue staining in developing embryos of three independent *CrLFY1*$_{pro}$*::GUS* transgenic reporter lines (**A–O**), a representative negative wild-type control line (**P–T**) and a representative positive *35S*$_{pro}$*::GUS* control line (**U–Y**). Tissues are shown prior to fertilization (**A, F, K, P, U**), or 2 (**B, G, L, Q, V**), 4 (**C, H, M, R, W**), and 6 (**D, I, N, S, X**) days after fertilization (DAF). In *CrLFY1*$_{pro}$*::GUS* lines, GUS activity first became visible within the first few divisions of embryo development (but not in surrounding gametophyte tissues) at 2 DAF (**B, G, L**) and was expressed in cells of the embryo frond as it proliferated (**C, H, M**). GUS activity was visible in the shoot apex and in frond vascular tissue at 6 DAF (**D, I, N**), with staining in the shoot apical cell (sac), subtending shoot apex tissues and newly-initiated fronds, including the frond apical cell (fac) (**E, J, O**). No GUS activity was detected in wild-type samples (**P–T**), whereas the majority of cells in the constitutively expressing *35S*$_{pro}$*::GUS* samples stained blue (**U–Y**). Embryos develop on the surface of the gametophyte thallus when an egg cell (ec) within the archegonium (which comprises a venter (**v**) and neck cells (nc) to allow sperm

Figure 4 continued on next page

Figure 4 continued

entry) are fertilized. After fertilization, the venter forms a jacket of haploid cells known as the calyptra (**c**) that surrounds the diploid embryo (em). Cell fates in the embryo (embryo frond (fr), embryo foot (ft), root apex (ra) and shoot apex (sa)) are established at the eight-celled stage (***Johnson and Renzaglia, 2008***), which is around 2 DAF under our growth conditions. Embryogenesis is complete at 6 DAF, after which fronds arise from the shoot apex. Scale bars = 50 μm.

DOI: https://doi.org/10.7554/eLife.39625.009

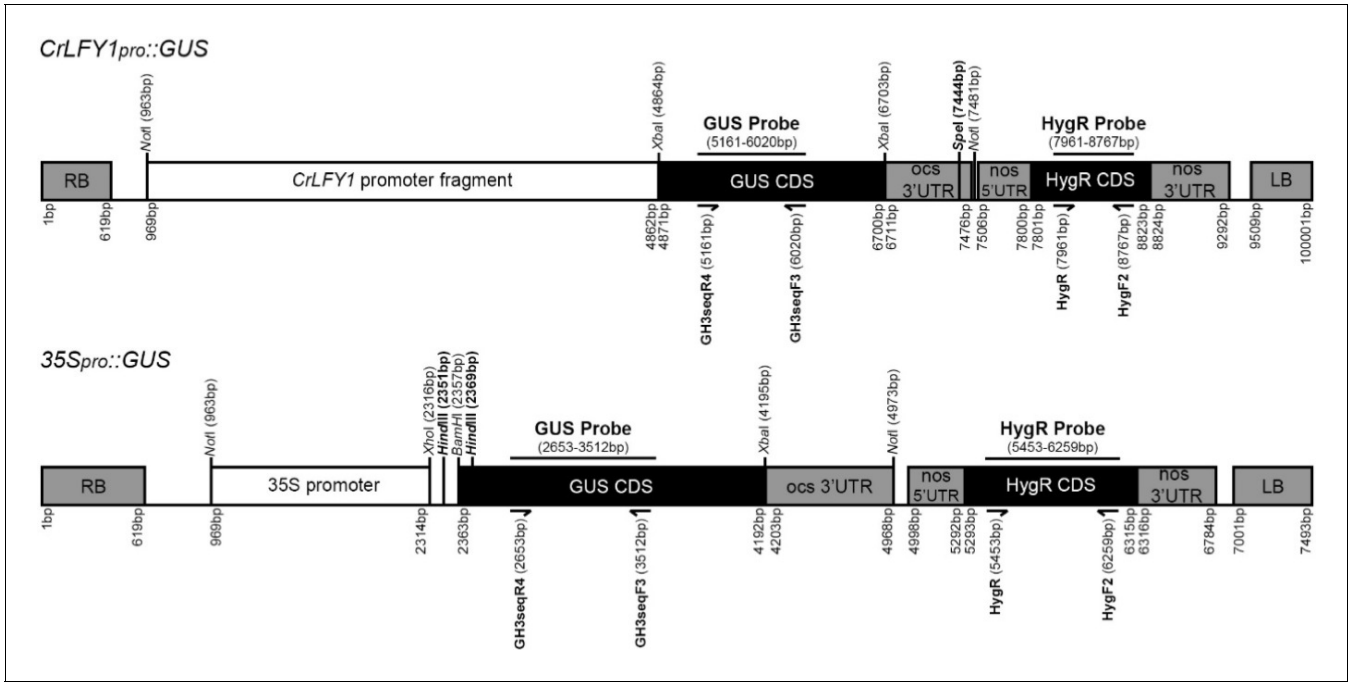

Figure 4—figure supplement 1. Schematic of *CrLFY1pro::GUS* and *35S$_{pro}$::GUS* constructs. Hybridization probes for the GUS and hygromycin resistance (HygR) genes, plus the position of the *Spe*I and *Hind*III restriction sites used for DNA gel blot analysis (***Figure 4—figure supplement 2***) are indicated. Restriction sites used in plasmid construction (see Materials and methods) are also indicated. All nucleotide positions are given relative to the start of the T-DNA right border (RB). Primer sequences are listed in the Key Resources Table.

DOI: https://doi.org/10.7554/eLife.39625.010

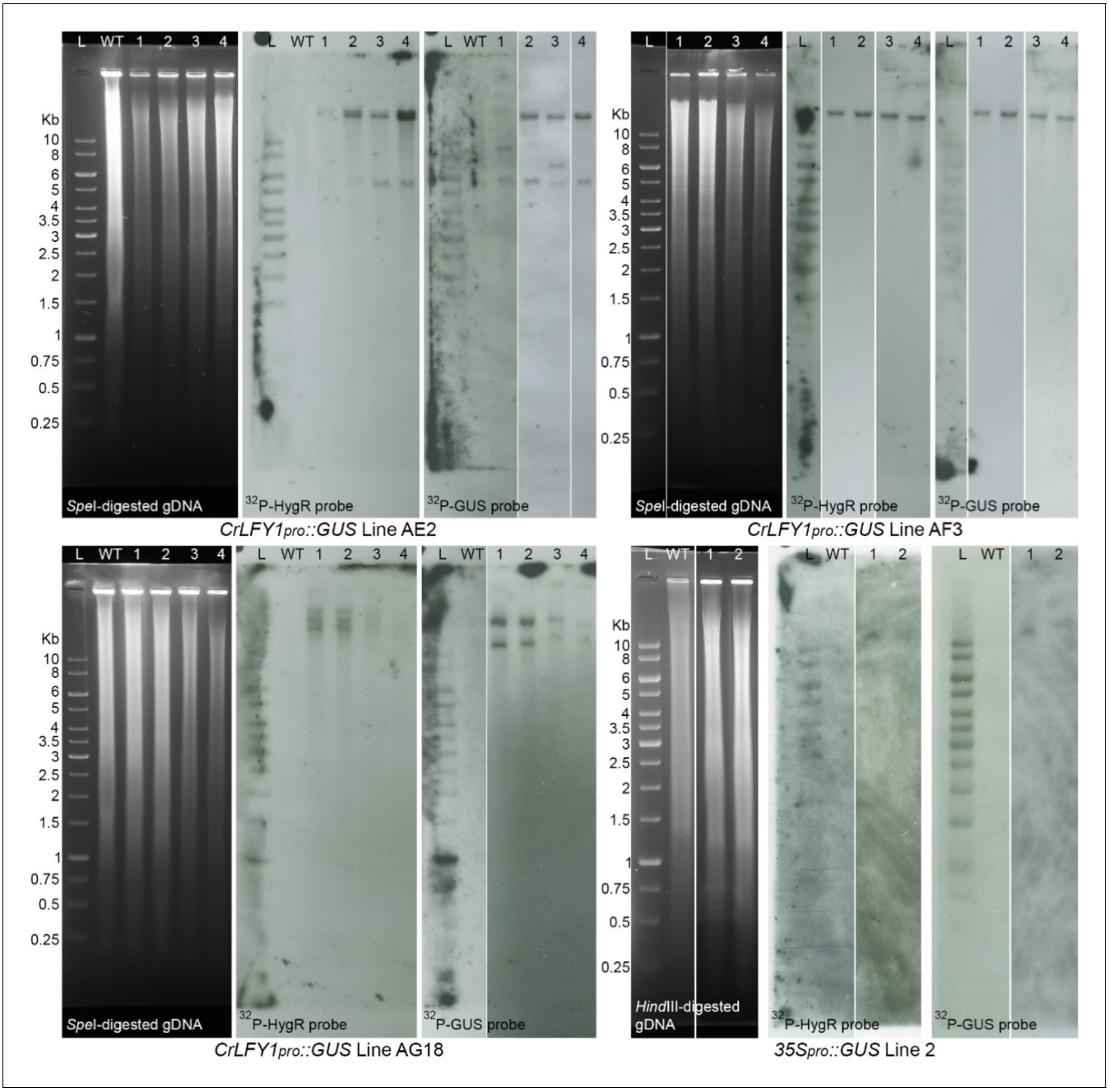

Figure 4—figure supplement 2. DNA gel blot analysis of *CrLFY1*$_{pro}$*::GUS* and *35S*$_{pro}$*::GUS* transgenic lines. *CrLFY1*$_{pro}$*::GUS* lines AE2, AF3, and AG18 were regenerated from three separate bombardments and so are necessarily independent of one another. Genomic DNA was extracted from four T_1 sporophytes (arising from the free fertilization of T_1 gametophytes) within each line, digested with *SpeI* and separated on an electrophoresis gel. Genomic DNA from two T_1 sporophytes of *35S*$_{pro}$*::GUS* line two was digested with *Hind*III. Gel blot analysis of both constructs was performed with the same two probes, hybridizing to the GUS CDS and hygromycin resistance (HygR) CDS, respectively (***Figure 4—figure supplement 1***). For each full-length *CrLFY1*$_{pro}$*::GUS* T-DNA insertion present in the genome a single insert is predicted to result in unlinked hybridization fragments with minimum sizes of ~2.5 kb (HygR) and ~6 kb (GUS). For *35S*$_{pro}$*::GUS*, a single fragment with a minimum size of ~5.1 kb is predicted per insertion event for both probes (see ***Figure 4—figure supplement 1***). Gel blot results indicate the presence of one full-length T-DNA insertion in *35Spro::GUS* line 2. Based on the hybridization fragments obtained, *CrLFY1*$_{pro}$*::GUS* line AE2 contains two potentially full-length insertions of the *CrLFY1pro::GUS* cassette and 1–2 insertions of partial fragments, AF3 contains a single potential full length insertion and AG18 contains two potential full length insertions.

DOI: https://doi.org/10.7554/eLife.39625.011

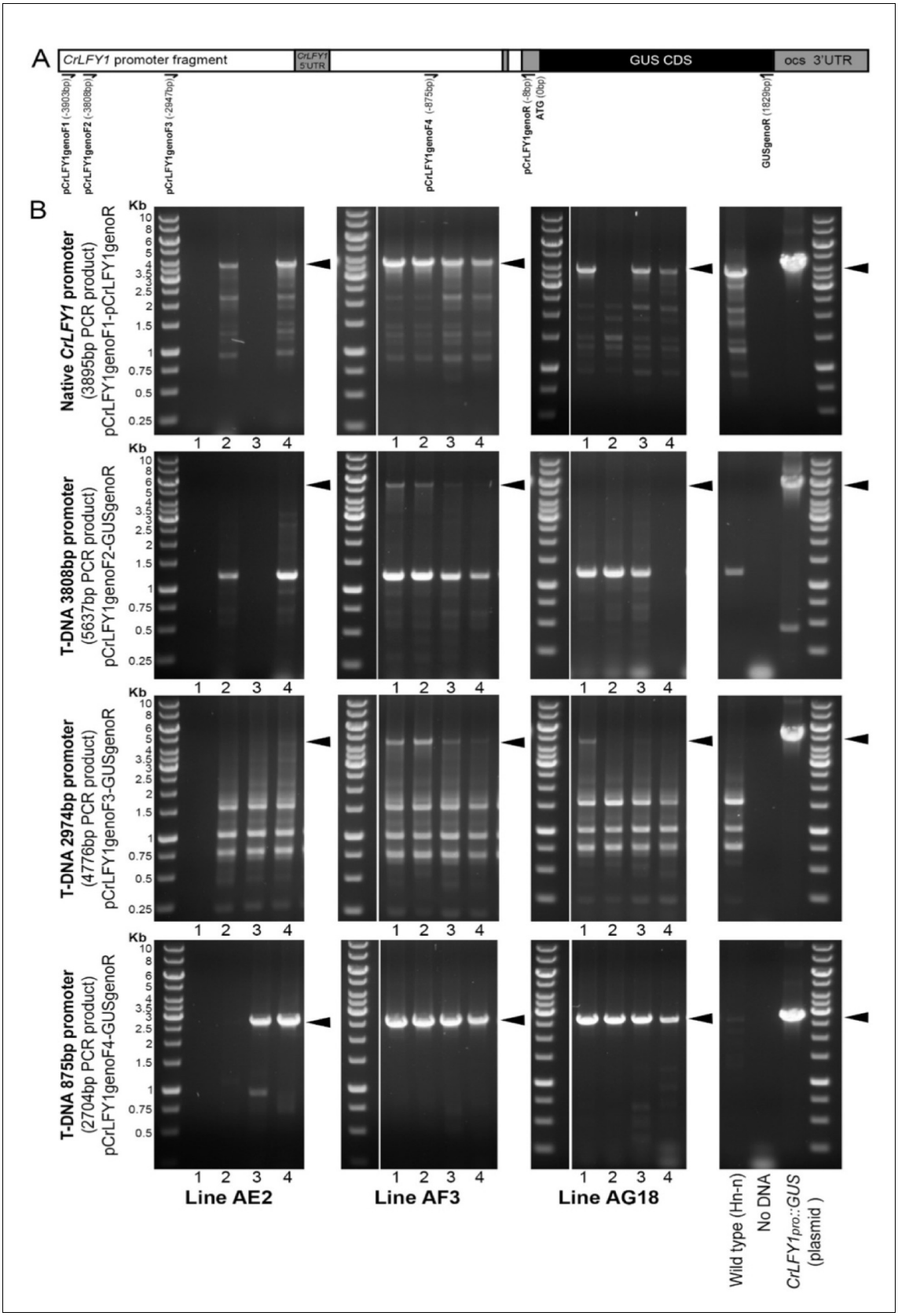

Figure 4—figure supplement 3. PCR analysis of *CrLFY1*$_{pro}$*::GUS* T_1 lines identified full-length or near full-length *CrLFY1* promoter sequences in T-DNA insertions. (**A**) Schematic of the *CrLFY1*$_{pro}$*::GUS* construct marking binding sites of PCR primers used in (**B**). All positions are given relative to the GUS

Figure 4—figure supplement 3 continued on next page

Figure 4—figure supplement 3 continued

ATG. Primer sequences are listed in the Key Resources Table. (**B**) PCR was performed on genomic DNA from the same four individual T_1 sporophytes within each line investigated by gel blot analysis (see ***Figure 4—figure supplement 2***). PCR reactions were performed to amplify the native 3.9 kb *CrLFY1* promoter as a positive control (row 1) and to amplify T-DNA specific products (rows 2–4) containing the GUS CDS and different lengths of contiguous *CrLFY1* promoter sequence (see **A**). Black arrowheads mark the expected size of the target PCR product in each reaction. PCR analysis identified at least one full-length GUS CDS with ~3.8 kb of *CrLFY1* promoter in line AF3 (row 2). Faint PCR products indicate that line AG18 and AE2 probably contain a full-length GUS CDS plus ~3 kb of *CrLFY1* promoter sequence (row 3). All lines carry a GUS CDS plus a minimum *CrLFY1* promoter length of 875 bp (row 4).

DOI: https://doi.org/10.7554/eLife.39625.012

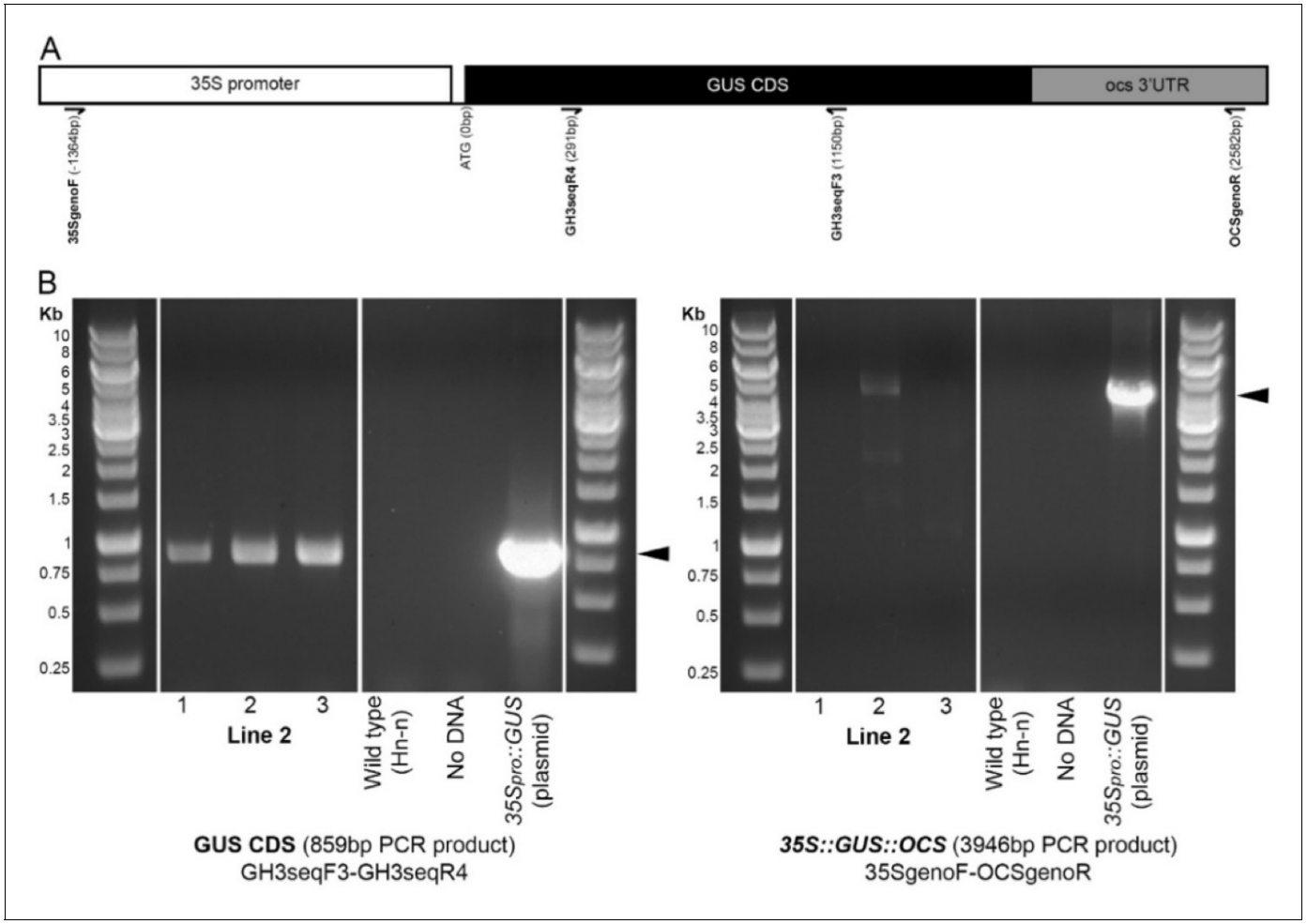

Figure 4—figure supplement 4. PCR analysis of *35S$_{pro}$::GUS* positive control line identified a full-length *35S$_{pro}$::GUS* insertion. (**A**) Schematic of the *35S$_{pro}$::GUS* construct marking binding sites of genotyping primers used in (**B**). All positions shown are relative to the GUS ATG. Primer sequences are listed in the Key Resoucres Table. (**B**) PCR was performed on genomic DNA extracted from three T_1 individuals, including the two investigated by gel blot analysis (***Figure 4—figure supplement 2***). T-DNA specific reactions were performed to amplify the GUS CDS (left) previously identified by gel blot analysis (***Figure 4—figure supplement 2***) using the same primers as the gel-blot probe, and a PCR product spanning almost the full length of the *35S::GUS::OCS* construct (right). Black arrowheads mark the expected size of the target PCR product in each reaction. PCR results indicate the presence of a full length *35S$_{pro}$::GUS* T-DNA in this line.

DOI: https://doi.org/10.7554/eLife.39625.013

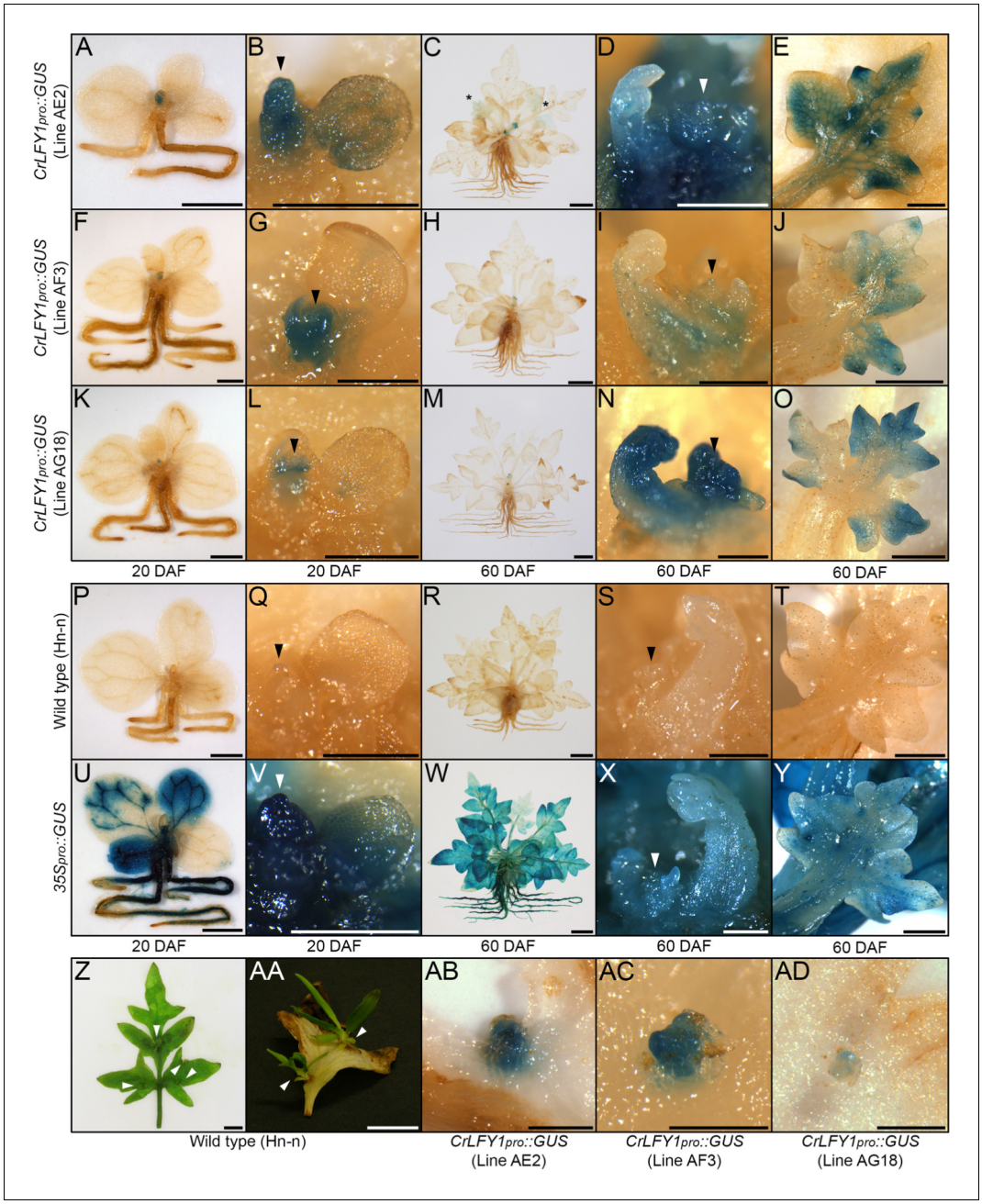

Figure 5. The *CrLFY1* promoter drives reporter gene expression in proliferating shoot tissues of the Ceratopteris sporophyte. (**A–Y**) GUS activity detected as blue staining in post-embryonic sporophytes from three independent *CrLFY1*$_{pro}$*::GUS* transgenic reporter lines (**A–O**), negative wild-type controls (**P–T**) and positive *35S*$_{pro}$*::GUS* controls (**U–Y**). Sporophytes were examined at 20 DAF (**A, B, F, G, K, L, P, Q, U, V**) and 60 DAF (**C–E, H–J, M–O, R–T, W–Y**). GUS staining patterns are shown for whole sporophytes (**A, C, F, H, K, M, P, R, U, W**), shoot apices (arrowheads) (**B, D, G, I, L, N, Q, S, V, X**) and developing fronds (**E, J, O, T, Y**). In *CrLFY1*$_{pro}$*::GUS* sporophytes at 20 DAF (producing simple, spade-like fronds) GUS activity was restricted to the shoot apex (**A, F, K**) and newly-initiated frond primordia, with very low activity in expanded fronds (**B, G, L**). In *CrLFY1*$_{pro}$*::GUS* sporophytes at 60 DAF (producing complex, highly dissected fronds) GUS activity was similarly seen in the apex (**C, H, M**), but persisted for longer during frond development. Activity was initially detected throughout the frond primordium (**D, I, N**), before becoming restricted to actively proliferating areas of the lamina (**E, J, O**). Scale bars = 2 mm (**A, F, K, P, U**), 500 µm (**B, D, G, I, L, N, Q, S, V, X**) 10 mm (**C, H, M, R, W**), 1 mm (**E, J, O, T, Y**). *=GUS staining in maturing frond. GUS staining patterns were the same in leaves formed after the reproductive transition (***Figure 5—figure supplement 1***). (**Z-AD**) Fronds can initiate *de novo* shoots (white arrowheads) from marginal tissue between

Figure 5 continued on next page

Figure 5 continued

existing frond pinnae (**Z, AA**). GUS activity was detected in emerging de novo shoot apices on *CrLFY1*$_{pro}$*::GUS* fronds (**AB–AD**). Scale bars = 10 mm (**Z, AA**), 500 µm (**AB–AD**).

DOI: https://doi.org/10.7554/eLife.39625.014

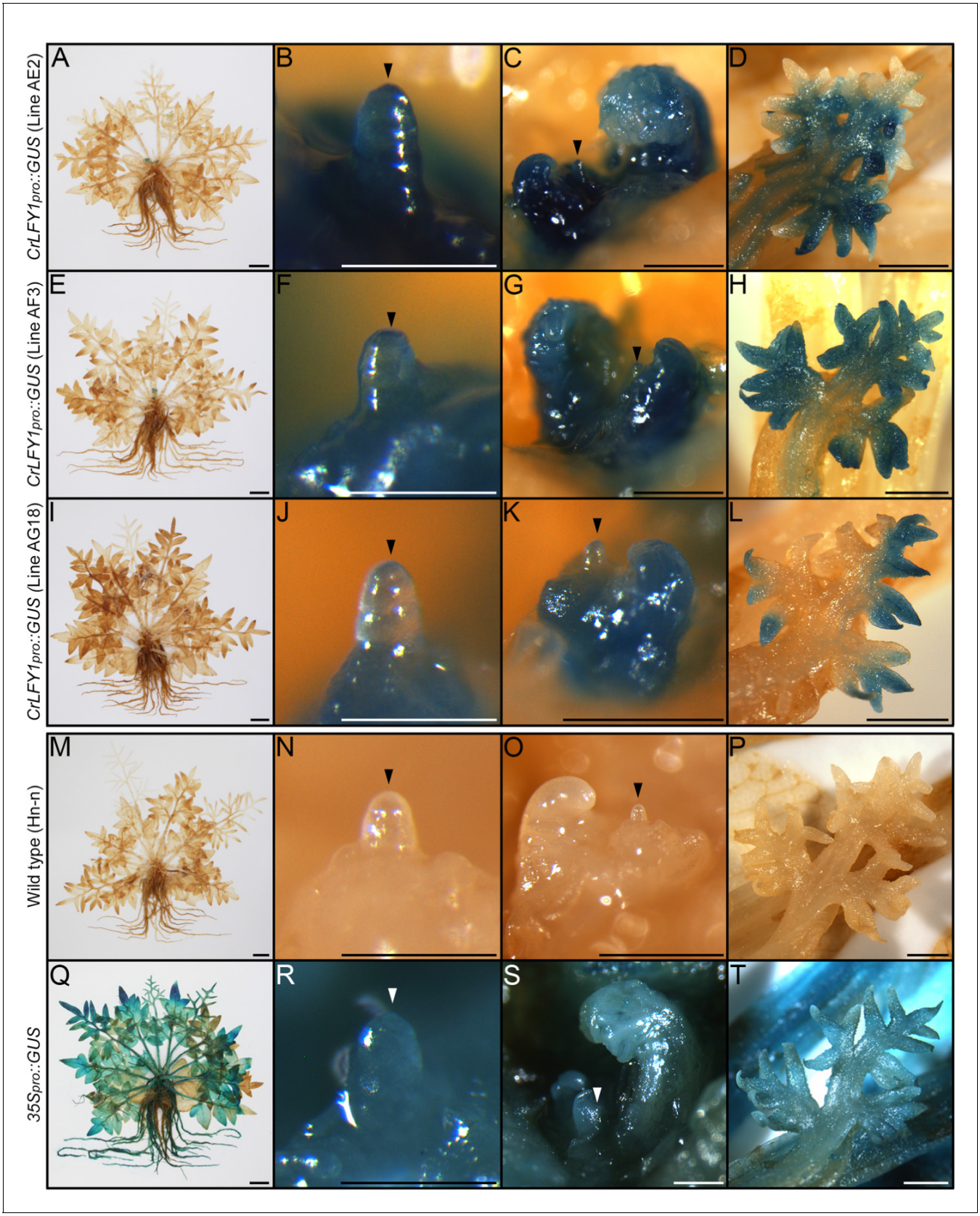

Figure 5—figure supplement 1. *CrLFY1*$_{pro}$*::GUS* expression patterns are similar in Ceratopteris shoots before and after reproductive phase change. GUS activity detected as blue staining in sporophytes producing fronds with spore-bearing morphology (narrowing and elongation of pinnae) from

Figure 5—figure supplement 1 continued on next page

Figure 5—figure supplement 1 continued

three independent *CrLFY1*$_{pro}$*::GUS* transgenic reporter lines (**A–L**); 110–124 DAF), negative wild-type controls (**M–P**); 113 DAF) and positive *35S*$_{pro}$*::GUS* controls (**Q–T**); 110 DAF). Staining patterns were consistent between the three independent *CrLFY1*$_{pro}$*::GUS* transgenic lines (**A, E, I**), and were similar to those seen at 60 DAF (***Figure 4C, (H,M***). GUS activity was observed throughout the shoot apex (**B, F, J**) and in recently-emerged frond primordia (**C, G, K**). Activity persisted later in frond development, becoming restricted to developing pinnae (**D, H, L**). GUS staining was lost from fronds prior to maturity (**A, E, I**). No endogenous GUS activity was detected in wild-type controls (**M–P**) whereas activity was detected throughout all non-senescent tissues in the *35S*$_{pro}$*::GUS* line (**Q–T**).

DOI: https://doi.org/10.7554/eLife.39625.015

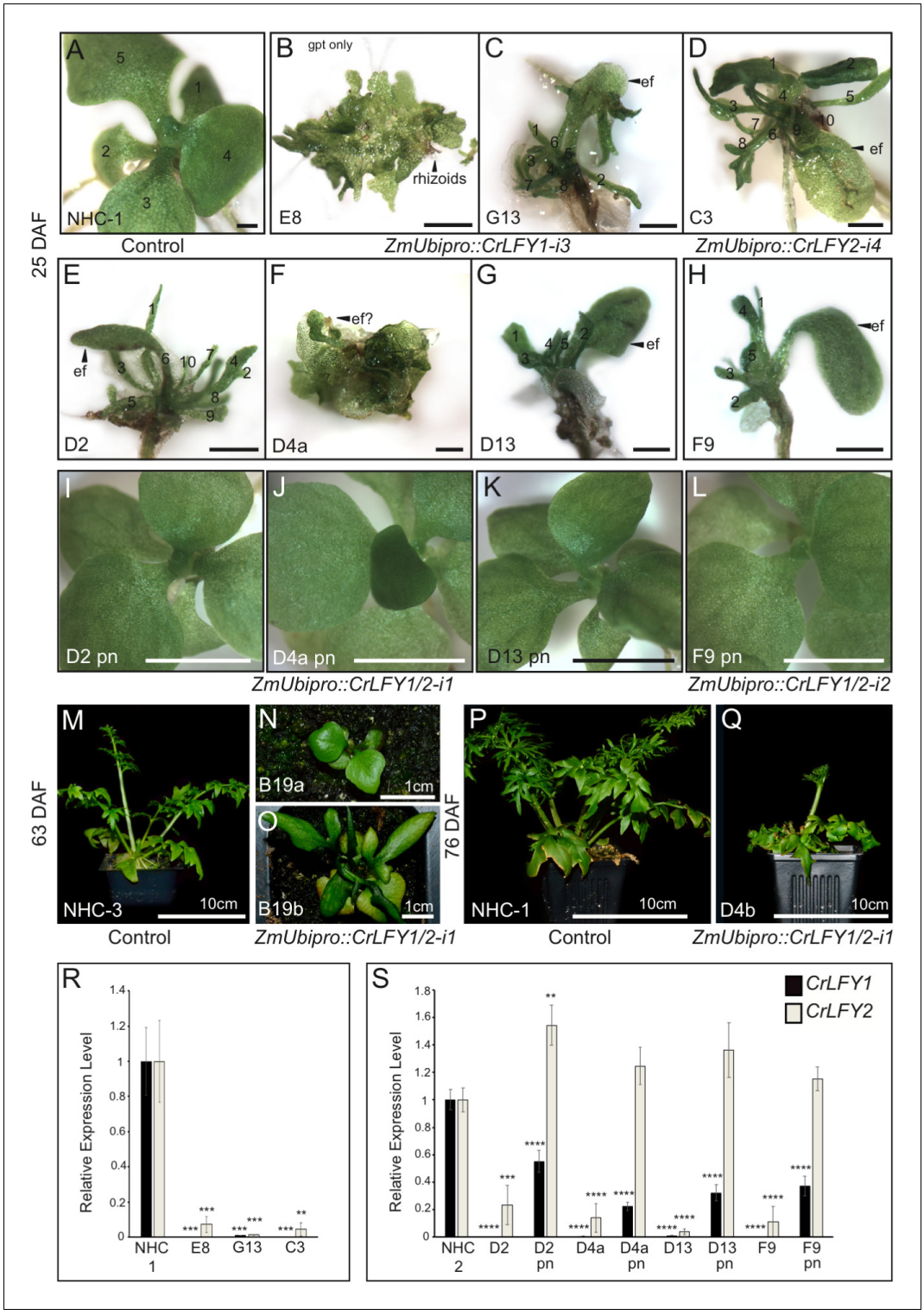

Figure 6. Suppression of *CrLFY* expression causes early termination of the Ceratopteris sporophyte shoot apex. (**A-L**) Sporophyte phenotype 25 days after fertilization (DAF) in no hairpin control, NHC-1 (**A**) and transgenic lines carrying RNAi constructs against *CrLFY1* (*ZmUbi$_{pro}$::CrLFY1-i3*) (**B, C**), *CrLFY2* (*ZmUbi$_{pro}$::CrLFY1-i4*) (**D**) and both *CrLFY1* and *CrLFY2* (*ZmUbi$_{pro}$::CrLFY1/2-i1* and *ZmUbi$_{pro}$::CrLFY1/2-i2*) (**E–L**). In some lines, both aborted and phenotypically normal sporophytes were identified (compare **E** and **I**; **F** and **J**; **G** and **K**; **H** and **L**). The presence of the RNAi transgene in phenotypically normal sporophytes was validated by genotyping (***Figure 6—figure supplement 5***). Scale bars = 1 mm (**A–H**), 5 mm (**I–L**). (**M–Q**) Sporophyte phenotype of two no hairpin control

Figure 6 continued on next page

Figure 6 continued

(NHC-3 and NHC-1) (**M, P**) and two *ZmUbi$_{pro}$::CrLFY1/2-i1* (**N, O**) lines at 63 (**M–O**) and 76 (**P,Q**) DAF. (**R, S**) qRT-PCR analysis of *CrLFY1* and *CrLFY2* transcript levels (normalized against the averaged expression of reference genes *CrACTIN1* and *CrTBP*) in the sporophytes of the RNAi lines shown in (**A–L**). Transcript levels are depicted relative to no hairpin controls (NHC-1or −3), *n* = 3, error bars = standard error of the mean (SEM). *CrLFY1* and *CrLFY2* expression levels were significantly reduced compared to controls (p<0.01 or less) in all transgenic lines where sporophyte shoots undergo early termination (**A–H**), but in phenotypically normal (pn) sporophytes segregating in the same lines (**I–L**), only *CrLFY1* transcript levels were reduced (p<0.0001). *CrLFY2* transcript levels in pn sporophytes were not significantly lower than in controls. Asterisks denote level of significant difference from controls (**p<0.01, ***p<0.001; ****p<0.0001).

DOI: https://doi.org/10.7554/eLife.39625.017

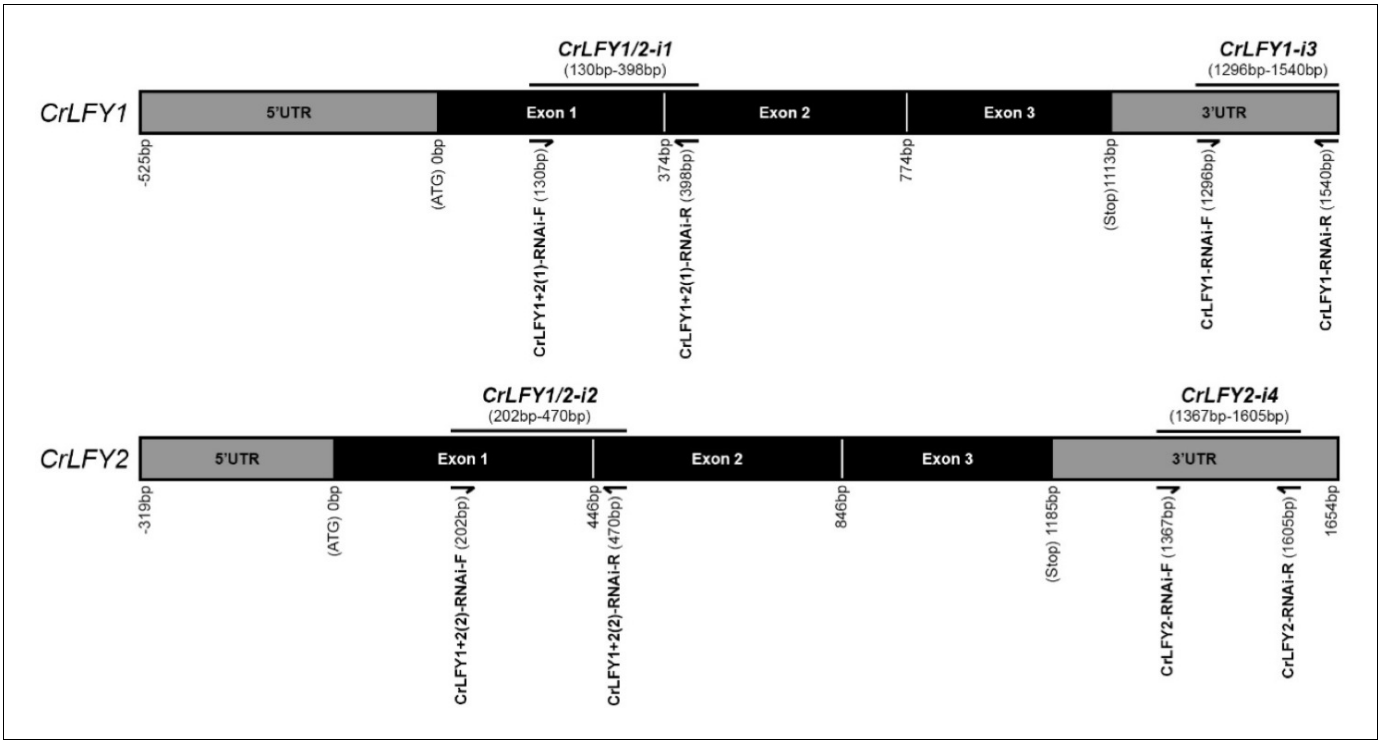

Figure 6—figure supplement 1. Positions of *CrLFY* RNAi target sequences. Schematic of *CrLFY1* and *CrLFY2* transcripts, showing recognition sequences used in RNAi constructs (black bars). 5′ and 3′ untranslated regions (UTRs) are marked by grey boxes, coding sequence (CDS) by black boxes, with exons as indicated. Positions are given relative to the translational start codon of each transcript. Four RNAi constructs were generated Two of these (*ZmUbi$_{pro}$::CrLFY1/2-i1* and *ZmUbi$_{pro}$::CrLFY1/2-i2*) targeted both *CrLFY1* and *CrLFY2* using conserved coding sequence amplified from *CrLFY1* (*ZmUbi$_{pro}$::CrLFY1/2-i1*) or *CrLFY2* (*ZmUbi$_{pro}$::CrLFY1/2-i2*). The two remaining constructs (*ZmUbi$_{pro}$::CrLFY1-i3* and *ZmUbi$_{pro}$::CrLFY2-i4*) incorporate target sequence amplified from the 3′UTR region of *CrLFY1* and *CrLFY2*, respectively. The position of primers used in target sequence amplification are shown. Primer sequences are supplied in the Key Resources table.

DOI: https://doi.org/10.7554/eLife.39625.018

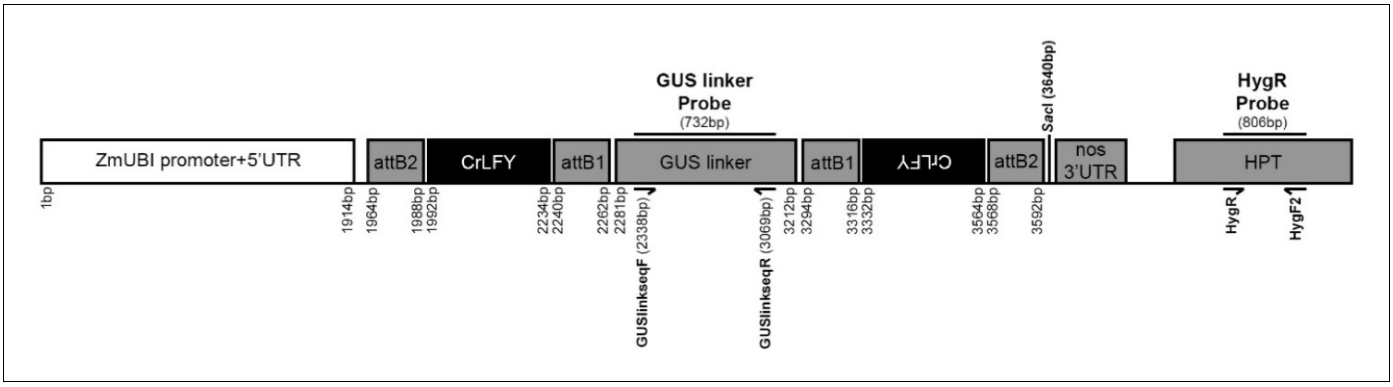

Figure 6—figure supplement 2. Generalized schematic of *CrLFY* RNAi constructs. Each RNAi construct carries inverted repeats of *CrLFY*-derived sequence (see ***Figure 6—figure supplement 1*** and ***Supplementary file 5***) to generate a hairpin bridged by a linker sequence derived from the GUS CDS (***Miki and Shimamoto, 2004***). The positions given are relative to the start of the maize ubiquitin promoter (*ZmUbi*$_{pro}$) that is driving RNAi expression, and are shown for *ZmUbi*$_{pro}$*::CrLFY1-i3*, with the length of the RNAi target sequence varying between the four different constructs (see ***Figure 6—figure supplement 1***). The sites of hybridization against probes for the GUS linker and hygromycin resistance marker (HygR) are shown. The position of a *Sac*I restriction site (used in gel blot analysis, see ***Figure 6—figure supplement 3***) is indicated. No *Sac*I sites are present in any *CrLFY* target sequence used. The primers used in probe amplification are given in the Key Resources Table.

DOI: https://doi.org/10.7554/eLife.39625.019

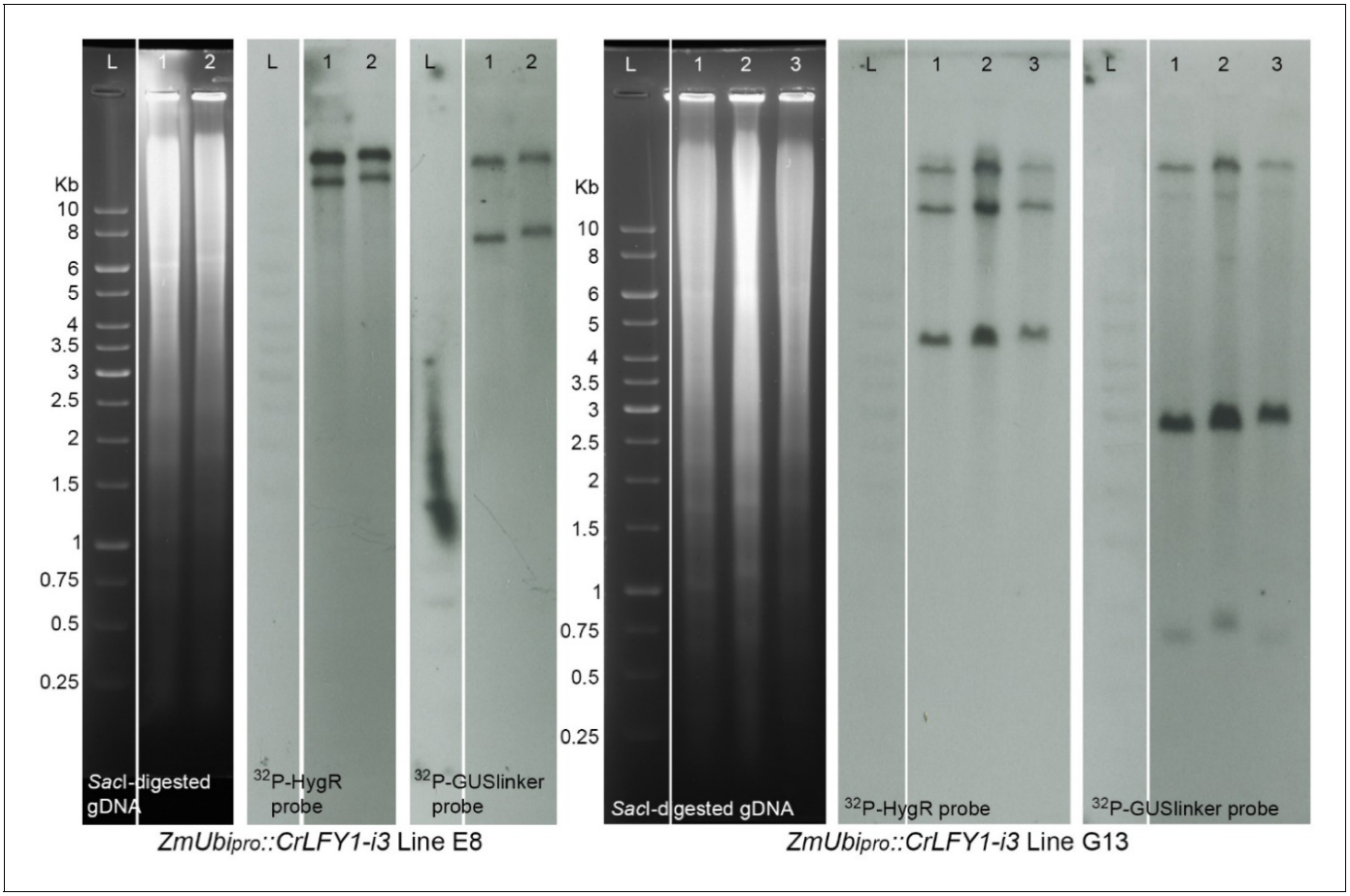

Figure 6—figure supplement 3. Gel blot analysis of *ZmUbi*$_{pro}$*::CrLFY1-i3* T_1 transgenic lines. *ZmUbi*$_{pro}$*::CrLFY1-i3* lines E8 and G13 were regenerated from two separate bombardments and so are necessarily independent of one another. Genomic DNA was extracted from four T_1 sporophytes (arising from the free fertilization of T_1 gametophytes) within each line, digested with *Spe*I and separated on an electrophoresis gel. Gel blot analysis of both constructs was performed with probes hybridizing either to the GUS linker of the RNAi hairpin or to the hygromycin resistance (HygR) CDS (***Figure 6—figure supplement 2***). For each full-length *ZmUbi*$_{pro}$*::CrLFY1-i3* T-DNA insertion present in the genome a single insert is predicted to result in unlinked hybridization fragments with minimum sizes of ~1 kb (HygR) or ~3.6 kb (GUS linker). Based on the hybridization fragments obtained, line E8 carries two full-length insertions of the *CrLFY1* RNAi cassette and line G13 carries two full-length insertions plus two additional partial insertions.

DOI: https://doi.org/10.7554/eLife.39625.020

A

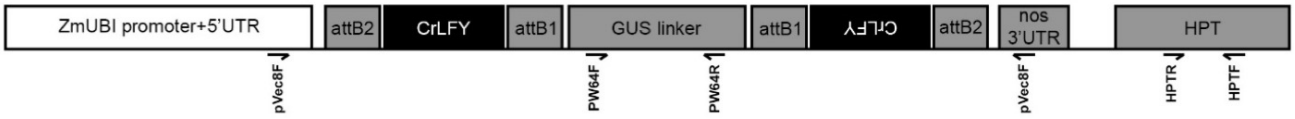

B

Genotyping Target	PCR product size	Primer
HygR	453bp	HPT-F HPT-R
CrLFY-RNAi hairpin (left arm + GUS)	1213bp (*CrLFY1/2-i1*, *CrLFY1/2-i2*) 1186bp (*CrLFY1-i3*) 1182bp (*CrLFY2-i4*)	pVec8F PW64R
CrLFY-RNAi hairpin (GUS + right arm)	1320bp (*CrLFY1/2-i1*, *CrLFY1/2-i2*) 1293bp (*CrLFY1-i3*) 1289bp (*CrLFY2-i4*)	PW64F pVec8R

Figure 6—figure supplement 4. Binding site of *CrLFY* RNAi genotyping PCR primers. (**A**) Generalized schematic of *CrLFY* RNAi T-DNA with the relative position of primers used in genotyping PCR (see ***Figure 6—figure supplement 5***, ***Figure 7—figure supplement 1***) marked. The primer binding sites are common to all four RNAi constructs, with the size of the hairpin-containing PCR products varying due to the insertion of different *CrLFY* target sequences. (**B**) Primer combinations for each genotyping reaction and expected PCR product sizes for each *CrLFY* RNAi construct. Primer sequences are listed in the Key Resources Table.

DOI: https://doi.org/10.7554/eLife.39625.021

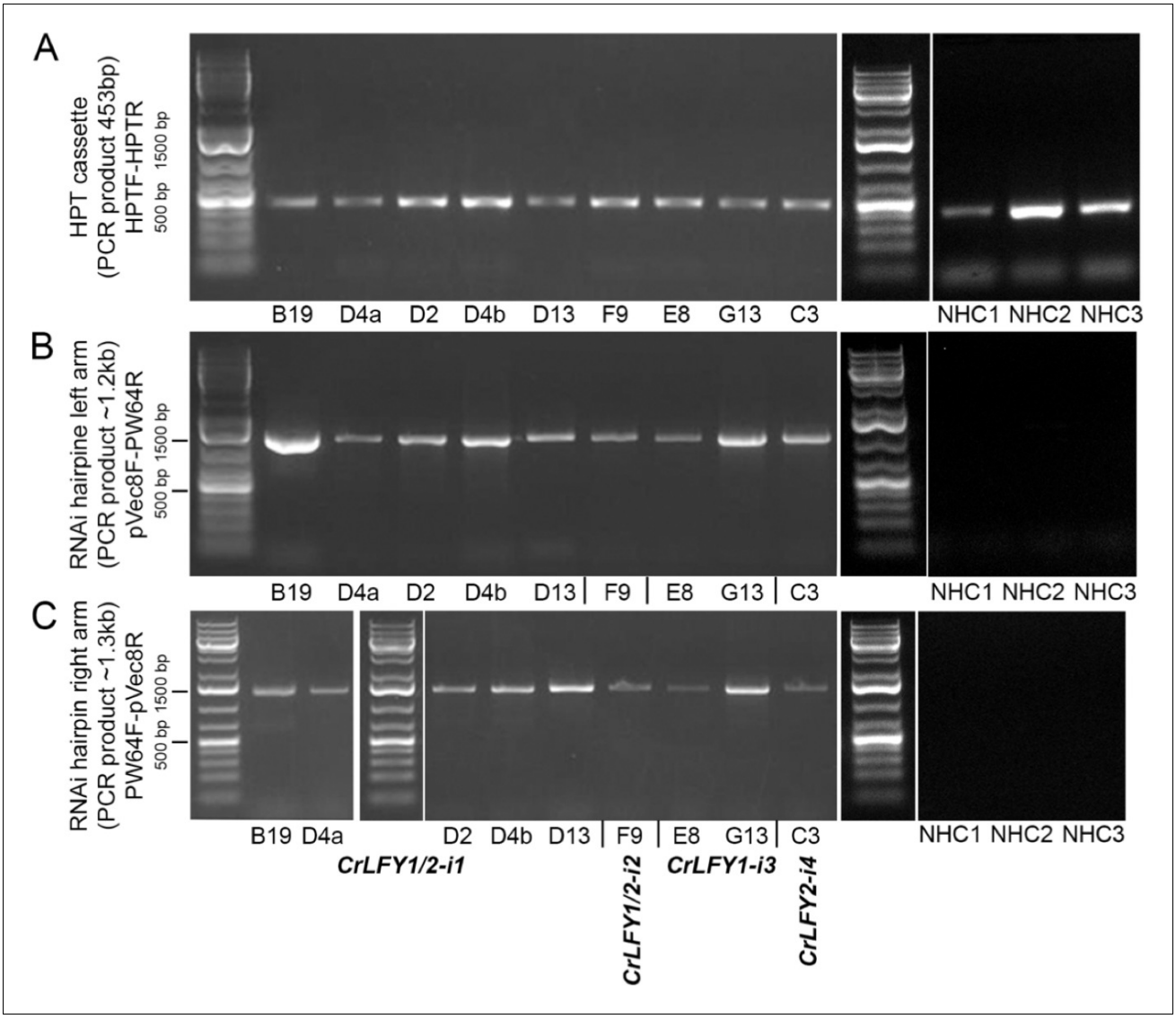

Figure 6—figure supplement 5. Genotyping PCR confirms the presence of *CrLFY* RNAi T-DNA in transgenic lines and the absence of the RNAi hairpin in no hairpin control lines. PCR was performed on genomic DNA extracted from T_1 sporophytes pre-selected for antibiotic resistance. The presence of the HPT cassette (**A**) was confirmed in all lines by PCR. The presence or absence of both arms of the RNAi hairpin (**B, C**) were confirmed in each line by PCR, and where sequenced the amplified products were as expected.

DOI: https://doi.org/10.7554/eLife.39625.022

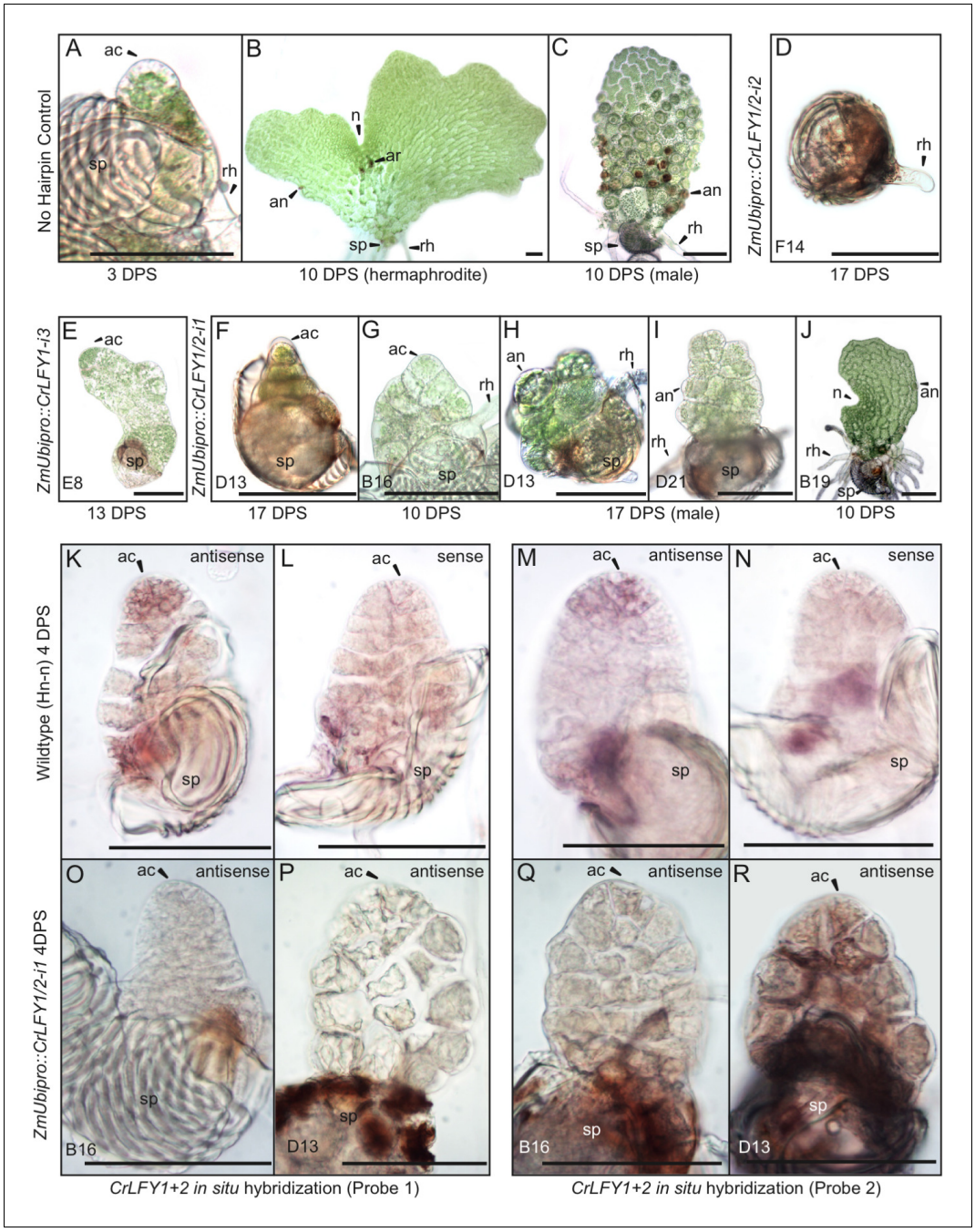

Figure 7. Suppression of *CrLFY* expression causes early termination of the Ceratopteris gametophyte apical cell. (**A–C**) In no hairpin control lines, the gametophyte established a triangular apical cell (ac) shortly after spore (sp) germination (**A**). Divisions of the apical cell established a photosynthetic thallus in both hermaphrodite and male gametophytes. At 10 days post spore sowing (DPS) both gametophyte sexes were approaching maturity, with the hermaphrodite (**B**) having formed a chordate shape from divisions at a lateral notch meristem (**n**) and having produced egg-containing archegonia (ar), sperm-containing antheridia (an), and rhizoids (rh). The male (**C**) had a more uniform shape with antheridia across the surface. These phenotypes were identical to wild-type. (**D–J**) When screened at 10–17 DPS, gametophytes from multiple RNAi lines (as indicated) exhibited developmental arrest, mostly associated with a failure of apical cell activity. Arrest occurred at various stages of development from failure to specify an apical cell, resulting in only a rhizoid being produced and no thallus (**D**) through subsequent thallus proliferation (**E–I**). Gametophyte development in one line progressed to initiation of the notch meristem but overall thallus size was severely reduced compared to wild-type (**J**). (**K–R**) In situ hybridization with antisense probes detected *CrLFY* transcripts in the apical cell and immediate daughter cells of wild-type gametophytes at 4

Figure 7 continued on next page

Figure 7 continued

DPS (**K, M**). No corresponding signal was detected in controls hybridized with sense probes (**L, N**). In the arrested gametophytes of two *ZmUbi*$_{pro}$*::CrLFY1/2-i1* lines *CrLFY* transcripts could not be detected (**O–R**), and transgene presence was confirmed (***Figure 7—figure supplement 1***). Scale bars = 100 µm.

DOI: https://doi.org/10.7554/eLife.39625.024

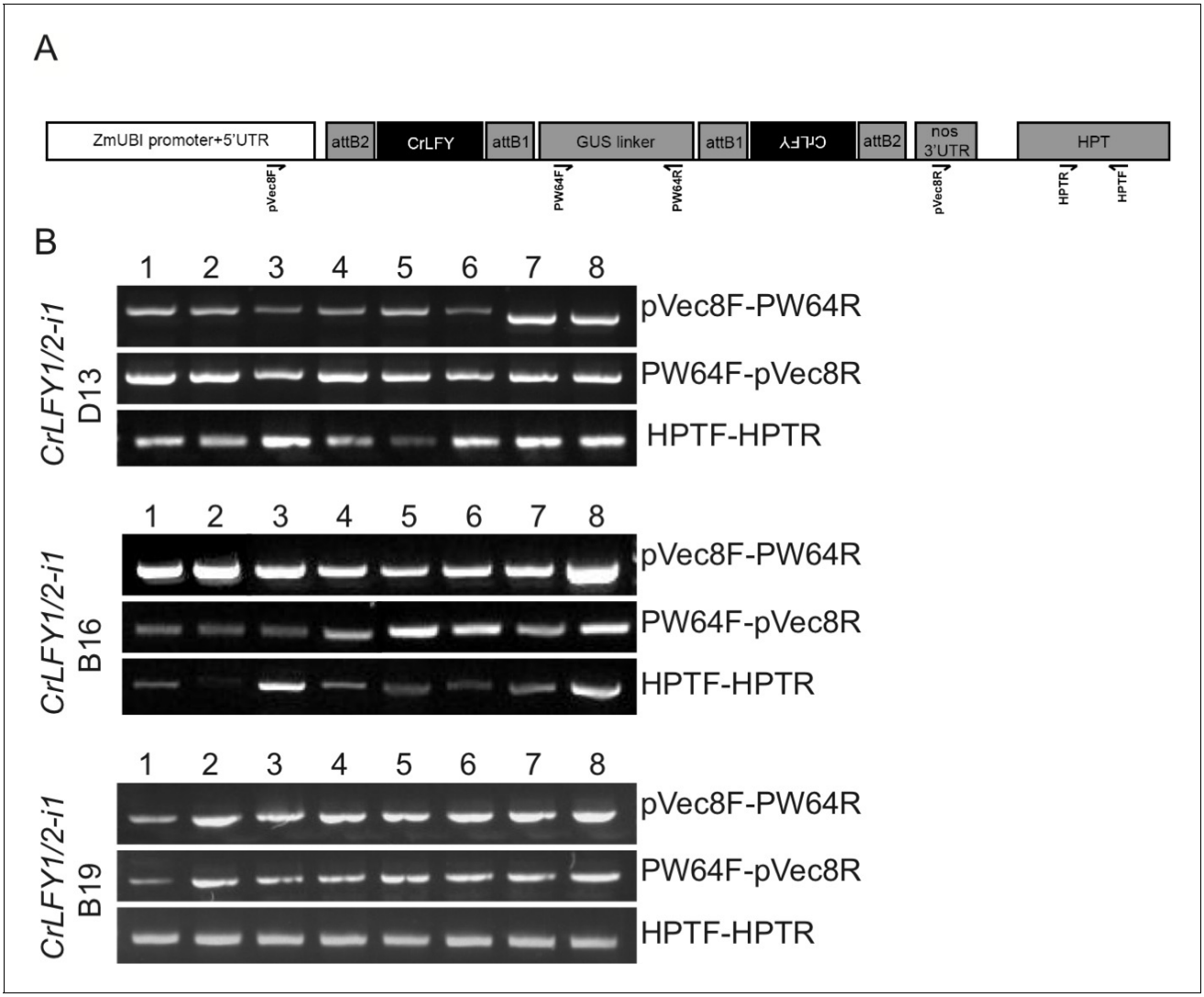

Figure 7—figure supplement 1. Gametophytes exhibiting developmental arrest were transgenic. **A**. Generalized schematic of *CrLFY* RNAi T-DNA with the relative position of primers used in genotyping PCR marked. Primer sequences and expected PCR product sizes for each *CrLFY* RNAi construct are given in ***Figure 6—figure supplement 4***. Genotyping PCR was conducted on DNA extracted from single gametophytes exhibiting developmental arrest at 10 DPS in three *ZmUbi*$_{pro}$*::CrLFY1/2-i1* lines. DNA from all arrested individuals amplified positive bands for the two hairpin arms (pVec8F-PW64R and PW64F-pVec8R) and for the hygromycin resistance marker (HPTF-HPTR).

DOI: https://doi.org/10.7554/eLife.39625.025

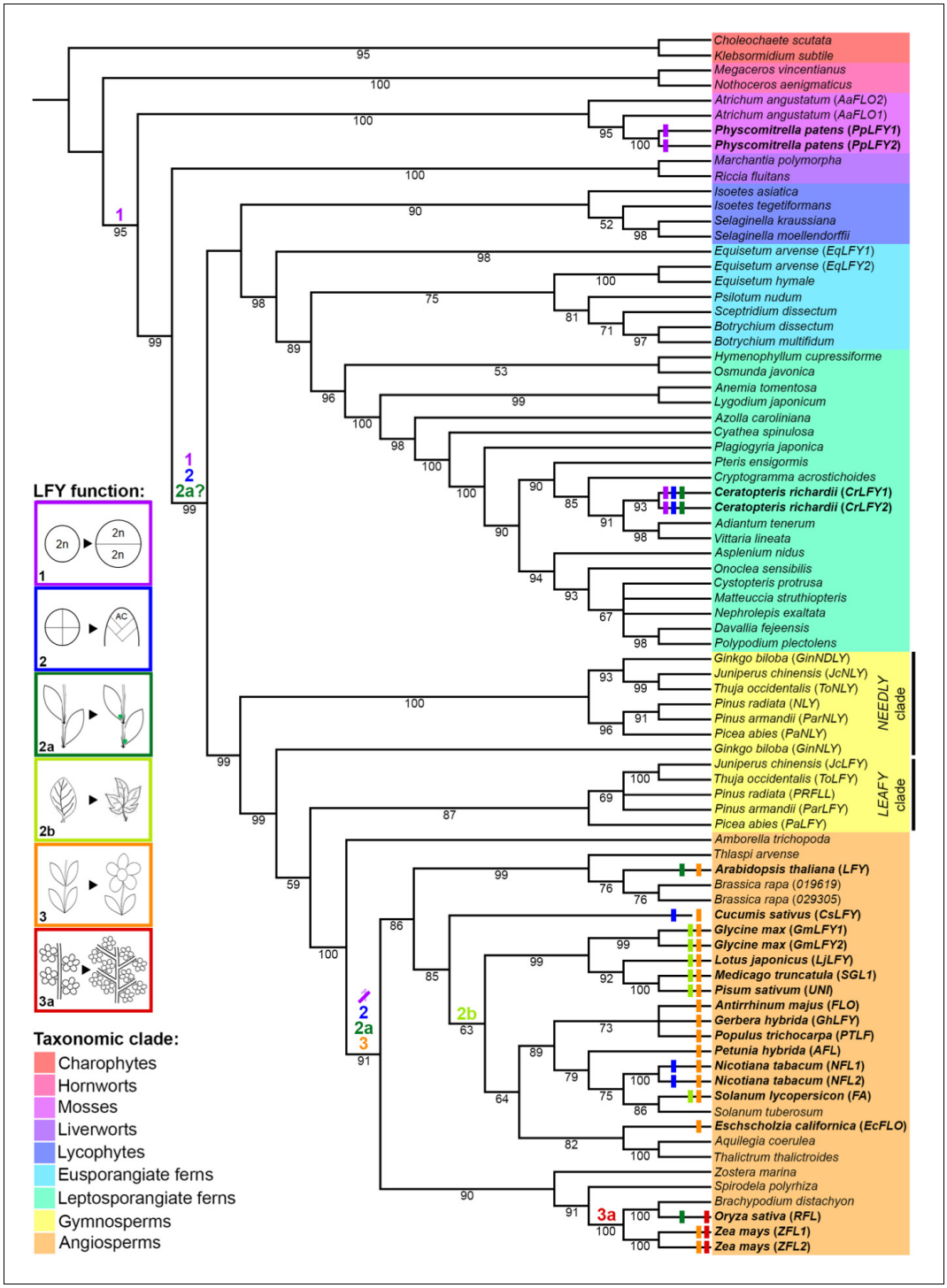

Figure 8. Evolutionary trajectory of LFY function. The phylogeny was reconstructed from selected LFY protein sequences representing all extant embryophyte lineages (as highlighted) and the algal sister-group. Coloured bars at the terminal branches represent different developmental functions of LFY determined from functional analysis in those species (see ***Supplementary file 8*** for references). Coloured numbers indicate the putative points of origin of different functions inferred from available data points across the tree. 1, cell division within the sporophyte zygote; 2, maintenance of indeterminate cell fate in vegetative shoots through proliferation of one or more apical cells (AC); 2a, maintenance of indeterminate cell fate in vegetative lateral/axillary apices; 2b, maintenance of indeterminate cell fate in the margins of developing lateral organs (compound leaves); 3, specification of floral meristem identity (determinate shoot development producing modified lateral organs) and shoot transition to the

Figure 8 continued on next page

Figure 8 continued

reproductive phase; 3a, maintenance of indeterminate cell fate in inflorescence lateral/branch meristems (in place of floral meristem fate).

DOI: https://doi.org/10.7554/eLife.39625.026